ARTICLE

Mutant GlialCAM Causes Megalencephalic Leukoencephalopathy with Subcortical Cysts, Benign Familial Macrocephaly, and Macrocephaly with Retardation and Autism

Tania López-Hernández,[1,9] Margreet C. Ridder,[3,9] Marisol Montolio,[1,4] Xavier Capdevila-Nortes,[1] Emiel Polder,[3] Sònia Sirisi,[1,6] Anna Duarri,[1,4] Uwe Schulte,[7] Bernd Fakler,[7] Virginia Nunes,[2,5,6] Gert C. Scheper,[3] Albert Martínez,[8] Raúl Estévez,[1,4,10,*] and Marjo S. van der Knaap[3,10,*]

Megalencephalic leukoencephalopathy with subcortical cysts (MLC) is a leukodystrophy characterized by early-onset macrocephaly and delayed-onset neurological deterioration. Recessive *MLC1* mutations are observed in 75% of patients with MLC. Genetic-linkage studies failed to identify another gene. We recently showed that some patients without *MLC1* mutations display the classical phenotype; others improve or become normal but retain macrocephaly. To find another MLC-related gene, we used quantitative proteomic analysis of affinity-purified MLC1 as an alternative approach and found that GlialCAM, an IgG-like cell adhesion molecule that is also called HepaCAM and is encoded by *HEPACAM*, is a direct MLC1-binding partner. Analysis of 40 MLC patients without *MLC1* mutations revealed multiple different *HEPACAM* mutations. Ten patients with the classical, deteriorating phenotype had two mutations, and 18 patients with the improving phenotype had one mutation. Most parents with a single mutation had macrocephaly, indicating dominant inheritance. In some families with dominant *HEPACAM* mutations, the clinical picture and magnetic resonance imaging normalized, indicating that *HEPACAM* mutations can cause benign familial macrocephaly. In other families with dominant *HEPACAM* mutations, patients had macrocephaly and mental retardation with or without autism. Further experiments demonstrated that GlialCAM and MLC1 both localize in axons and colocalize in junctions between astrocytes. GlialCAM is additionally located in myelin. Mutant GlialCAM disrupts the localization of MLC1-GlialCAM complexes in astrocytic junctions in a manner reflecting the mode of inheritance. In conclusion, GlialCAM is required for proper localization of MLC1. *HEPACAM* is the second gene found to be mutated in MLC. Dominant *HEPACAM* mutations can cause either macrocephaly and mental retardation with or without autism or benign familial macrocephaly.

Introduction

Megalencephalic leukoencephalopathy with subcortical cysts (MLC, MIM 604004) is a leukodystrophy with autosomal-recessive inheritance.[1] Patients develop macrocephaly during the first year of life. After several years, there is evidence of slow neurological deterioration, including cerebellar ataxia, spasticity, epilepsy, and mild cognitive decline. From early on, magnetic resonance imaging (MRI) reveals diffuse signal abnormality and swelling of the brain white matter and subcortical cysts (Figure S1, available online).[1] In follow-up exams, the white matter abnormalities remain and atrophy ensues.[1] A brain biopsy from an MLC patient showed extensive myelin vacuolation, mainly affecting the outer myelin layers, which causes the swollen appearance of the white matter.[2] In 2001, we demonstrated that mutations in *MLC1* (MIM 605908) cause MLC.[3] *MLC1* mutations are found in approximately 75% of the MLC patients.[4] MLC1 is an oligomeric membrane protein that is expressed almost exclusively in the brain. It has some degree of homology to ion channels.[5,6] Within the brain, MLC1 is mainly located in astrocyte-astrocyte junctions close to blood- and cerebrospinal fluid (CSF)-brain barriers, Bergmann glia, and main axonal tracts.[5–7] Thus far, the physiological role of MLC1 has remained unknown, and a suggested role in ion transport has not been confirmed.[3,5,8]

In some families, members with MLC do not have *MLC1* mutations, and these families do not show linkage to the *MLC1* locus, indicating that mutations in at least one other gene are involved in MLC,[9,10] but genetic-linkage studies failed to identify another disease gene. We recently described two distinct phenotypes among MLC patients without *MLC1* mutations.[11] The classical phenotype retains typical clinical and MRI features, as seen in patients with *MLC1* mutations.[1,11] The second, improving phenotype is initially the same as the classical phenotype but lacks clinical deterioration and shows major improvement or normalization of the MRI abnormalities (Figure S1).[11]

Because of the unsuccessful genetic-linkage studies and the possibility of further genetic heterogeneity, we decided to use alternative strategies to identify eligible candidate genes.

[1]Sección de Fisiología, [2]Sección de Genética, Departamento de Ciencias Fisiologicas II, University of Barcelona, 08907 Barcelona, Spain; [3]Department of Child Neurology, VU University Medical Center, De Boelelaan 1117, 1081 HV Amsterdam, The Netherlands; [4]Centro de Investigación en Red de Enfermedades Raras (CIBERER), U-750, [5]Centro de Investigación en Red de Enfermedades Raras (CIBERER), U-730, ISCIII, 08907 Barcelona, Spain; [6]Laboratorio de Genética Molecular-IDIBELL, 08907 Barcelona, Spain; [7]Logopharm GmbH, Engesserstrasse 4, 79108 Freiburg, Germany; [8]Department of Cell Biology, Faculty of Biology and Institute for Research in Biomedicine, University of Barcelona, 08907 Barcelona, Spain
[9]These authors contributed equally to this work
[10]These authors contributed equally to this work
*Correspondence: restevez@ub.edu (R.E.), ms.vanderknaap@vumc.nl (M.S.v.d.K.)
DOI 10.1016/j.ajhg.2011.02.009.

Material and Methods

The studies on human samples were performed with approval of the institutional review board, VU University Medical Center, Amsterdam, and informed consent from the families. The animal experimental protocols were approved by the Animal Care and Ethics Committee of the University of Barcelona. Protocols for the use and manipulation of the animals were approved by the Government of Catalonia.

Biochemistry

Preparation of Source Material

Plasma membrane-enriched protein fractions were prepared from pools of freshly isolated whole rat or mouse brains according to the procedure used in Zolles et al.[12] For solubilization, the prepared membrane vesicles were resuspended in ComplexioLyte buffer 47a (at 0.8 mg protein/ml, LOGOPHARM GmbH, Germany; with protease inhibitors added) and incubated for 30 min at 4°C; nonsoluble components were removed afterward by ultracentrifugation (10 min at 150.000 × g). Efficiency of solubilization was determined by immunoblot analysis of SDS-PAGE-resolved aliquots of solubilisate and pellet fractions. Polyvinylidene fluoride (PVDF) membranes were probed with rabbit polyclonal antibodies (α-N1 or α-NH, 1:10.000, see below), stained with goat anti-rabbit-HRP (Santa Cruz Biotechnologies, USA) and developed with ECL+ (GE Healthcare, USA).

Preparation of Antibodies

Immune sera against N-terminal mouse MLC1 peptides (α-N1 and α-N2) and the α-NH (anti-N-terminus of human MLC1) antibody were generated and characterized previously.[5,7,13] The α-NH also recognizes mouse/rat MLC1. Immune sera against a mouse GlialCAM synthetic peptide (QRIREQDESGQVEISA), corresponding to amino acids 403–418 of GlialCAM, were raised in rabbits with the help of the services provided by Eurogentec. The peptide was coupled to keyhole limpet hemocyanin via a cysteine residue that has been added to the N-terminal end of the peptide. After three boosts of immunization, the antisera were affinity purified with the peptide covalently coupled to Sulpholink (Pierce). The polyclonal antibody was tested by immunoblotting, immunofluorescence, and immunoprecipitation on HeLa cells expressing human GlialCAM and on mouse brain tissue.

Affinity Purification

For each experiment, 1.5 ml freshly prepared solubilisate (rat or mouse) was incubated for 2 hr at 4°C with 20 μg of the respective immobilized antibody[13] (*α-N1*, *α-N2* *α-NH*, *α-GlialCAM*, IgG = control rabbit IgG [Upstate, USA]). After a brief washing (twice for 5 min each time) with ComplexioLyte 47a, bound proteins were eluted with Laemmli buffer (dithiothreitol [DTT] was added after elution). Eluates were then briefly run on SDS-PAGE gels followed by silver staining and tryptic digestion. During these experiments, samples were taken for immunoblot analysis with the indicated MLC1 and GlialCAM antibodies.

Preparation of Myelin

Myelin was prepared as described previously.[14] Two brains from 6- to 8-week-old wild-type mice were homogenized in 20 volumes of homogenization buffer (0.32 M sucrose in 10 mM HEPES [pH 7.4]) with five strokes with a loose pestle and seven strokes with a tight pestle. The homogenate was layered over 0.85 M sucrose, centrifuged at 25,000 rpm for 30 min in a swinging bucket rotor. Proteins located in the interphase were removed, resuspended in 10 volumes of water, and centrifuged at 25,000 rpm for 15 min. The pellet was twice cleansed of sucrose by water suspension and centrifugation. Then, pellets were suspended again in homogenization buffer and layered over 0.85 M sucrose and centrifuged at 25,000 rpm for 30 min. The interphase layer was again suspended in water, centrifuged for 15 min, and resuspended in 10 mM HEPES buffer (pH 7.4) containing 1% Triton X-100. Protein was quantified by bicinchoninic acid, and 20 μg was used for SDS-PAGE and immunoblot analyses.

Mass Spectrometric Analysis

Liquid Chromatography-Mass Spectrometry/Mass Spectrometry Analysis

Stained gel lanes were excised in two parts (upper and lower), and proteins were digested with trypsin according to the procedure described previously.[15] Extracted peptides dissolved in 0.5% trifluoroacetic acid were loaded on a precolumn (C18 PepMap100, 5 μm; Dionex, Idstein, Germany) of an UltiMate 3000 HPLC (Dionex, Idstein, Germany). An aqueous organic gradient was then applied for elution and separation of peptides on a 75 μm column packed with C18 beads (ReproSil-Pur 120 ODS-3; Dr. A Maisch, Ammerbuch-Entringen, Germany) and directly electrosprayed into an LTQ-FT mass spectrometer (Thermo Scientific, Bremen, Germany; ion source: Proxeon, Odense, Denmark). Each scan cycle consisted of one FTMS full scan and up to five ITMS dependent MS/MS scans of the five most intense ions. Dynamic exclusion (30 s, mass width 20 ppm) and monoisotopic precursor selection were enabled. Using Mascot (Matrix Science, UK) we searched extracted MS/MS spectra against the Swiss-Prot database (*Mammalia*). We allowed common variable modifications and one missed tryptic cleavage; peptide tolerance was ± 10 ppm and MS/MS tolerance was ± 0.8 Da. Proteins that (1) were identified by only one specific MS/MS spectrum or (2) presented exogenous contaminations like keratins, trypsin, or immunoglobulins were not considered in further evaluations.

Protein Quantification

We used two previously detailed protein quantification methods[16] that are both based on liquid chromatography-mass spectrometry (LC-MS) peptide signal intensities extracted (as peak volumes [PVs]; m/z tolerance was 6 ppm) and aligned (between individual LC-MS runs by their retention times; tolerance was 8%) with MS Inspect (Computational Proteomics Laboratory, Fred Hutchinson Cancer Research Center, Seattle, WA, USA) and in-house written software. The *relative* quantity of a protein in affinity purification sample versus control was calculated as a median of consistent peak volume ratios of respective peptides (rPV). Ensuring the significance of rPVs, required that at least two peptide ratios had assigned PVs totaling 100,000 volume units. Proteins were regarded as specifically (co-) purified when their rPV values were higher than 10. The molar amounts of *different* proteins were compared by using $\text{abundance}_{\text{norm}}$ values (as in Figure 1), calculated as the sum of all assigned peak volumes (totalPV) divided by the number of MS-accessible amino acids (sequence of tryptic peptides with masses between 740 and 3000 Da under the MS settings used).

Genetic Analysis

The diagnosis of MLC was established by MRI criteria.[1] In those MLC patients in whom we found no mutations in *MLC1* by sequence analysis of genomic DNA, as well as analysis of *MLC1* cDNA and MLPA, we analyzed *HEPACAM* (hepatic and glial cell adhesion molecule, MIM 611642), the gene encoding GlialCAM. *HEPACAM* primers were designed with ExonPrimer (Table S1). Accession numbers of the reference sequences are NM_152722.4

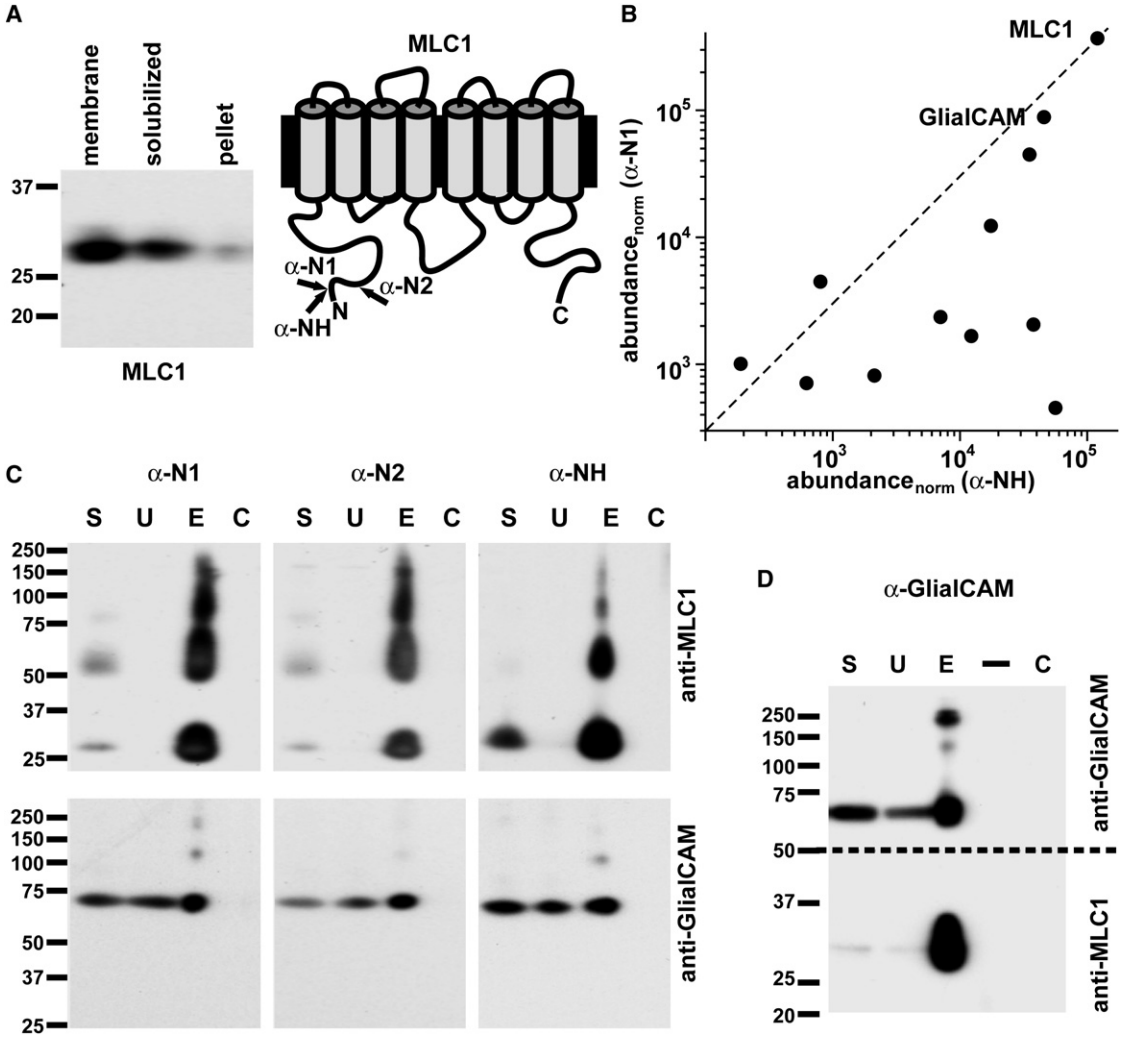

Figure 1. Proteomic Identification of GlialCAM as a Major Binding Partner of MLC1
(A) Affinity purification (AP) strategy based on efficient MLC1 solubilization (left) as visualized by immunoblot analysis of SDS-PAGE-resolved samples from rat brain membrane, solubilisate, and pellet (stained with anti-MLC1 (α-N1)) and three antibodies (right) directed against N-terminal epitopes of MLC1. Similar results were obtained when two different antibodies were applied or when the three antibodies were applied simultaneously, confirming the specificity of the proteomics data.
(B and C) Evaluation of MLC1 affinity purifications with the indicated antibodies. (B) 2D plot of protein abundances determined by mass spectrometry (for $abundance_{norm}$ values see Material and Methods) of AP with α-N1 (from rat brain) versus AP with α-NH (from mouse brain). Only proteins specifically enriched (more than 10-fold of the amount in the respective IgG control) and identified in both APs are shown (as dots). Note the distinct quantitative correlation of GlialCAM with MLC1. Pearson correlation of GlialCAM and MLC1 $abundance_{norm}$ values across all three APs and controls is $r = 0.96$. (C) Immunoblot analysis of APs with the indicated antibodies stained with anti-MLC1 (α-N1; upper) and anti-GlialCAM (lower); lanes resolve aliquots of solubilisate before (S) and after AP (U), of eluates from APs (E), and of corresponding IgG control APs (C).
(D) Immunoblots showing specific copurification of MLC1 in an AP with anti-GlialCAM (samples and antibodies labeled as before). "–" indicates no sample was loaded.

(mRNA) and NT_033899.8 (gDNA). PCR amplification of exons 1–6 of *HEPACAM* and their surrounding intronic regions was carried out with Platinum TAQ DNA Polymerase according to the manufacturer's instructions (Invitrogen). For exon 7, which has a very high-GC content, Platinum TAQ DNA-polymerase (Invitrogen) was used in combination with 5X AccuPrime™ GC-Rich Buffer A (Invitrogen). The PCR products were analyzed by cycle sequencing on an ABI3730 Genetic Analyzer (Applied Biosystems) with the same primers used for PCR amplification, with the exception of the forward primer of exon 1. The resulting chromatograms were analyzed with Sequence Pilot (JSI Medical Systems Gmbh) with ENSG00000165478 as reference sequence.

Immunofluorescent and Electron Microscopic Studies in Tissue
Tissue immunohistochemistry was performed as previously described.[5,7] For electron microscopic (EM) studies, small human cerebellum samples were obtained postmortem, fixed in 4% paraformaldehyde and 0.1% glutaraldehyde in 0.12 M phosphate buffer, and processed. They were cryoprotected gradually in sucrose and cryofixed by immersion in liquid propane. Freeze substitution was performed at −90°C during 3 days in an Automatic Freeze Substitution System (AFS, Leica); methanol containing 0.5% uranyl acetate was used as a substitution medium. Infiltration was carried out in Lowicryl HM20 at −50°C and then polymerized with UV lamps. Ultrathin sections were collected and processed for

postembedding immunostaining. For double immunostaining, grids were incubated with rabbit anti-N4-human MLC1 (1:10) and mouse anti-GlialCAM (1:10) antisera. The binding of primary antibodies was visualized by incubating with goat anti-rabbit or goat anti-mouse secondary antibodies conjugated to either 12 or 18 nm gold particles (British BioCell, International). In control experiments, the primary antibodies were omitted—no immunogold labeling occurred under these conditions.

Primary Culture and Adenoviral Transduction

Rat primary astrocytes were prepared as described previously[13] with some modifications. Cortex and hippocampus were removed from newborn (1 to 3 days old) Sprague Dawely rats (Charles River). Cerebral cortices were dissected and the meninges were carefully removed in cold sterile 0.3% BSA and 0.6% glucose in PBS. The tissue was trypsinized for 10 min at 37°C and mechanically dissociated in complete Dulbecco's modified Eagle's medium (DMEM; with 10% heat-inactivated fetal bovine serum [Biological Industries], 1% penicillin/streptomycin [Invitrogen] and 1% glutamine [Invitrogen] plus 40 U/ml DNase I [Sigma]) through a small bore fire-polished Pasteur pipette. The cell suspension was pelleted and resuspended in fresh complete DMEM, filtered through a 100-μm nylon membrane (BD Falcon) and plated into 75 cm^2 cell-culture flasks (TPP). When the mixed glial cells reached confluence, contaminating microglia, oligodendrocytes, and precursor cells were dislodged by mechanical agitation and removed as previously described.[17]

Astrocytes were plated in 6-well plates at a density of 4×10^5 cells per well or in poly-D-lysine-coated coverslips at 7.5×10^4 cells per 24-well plate. Medium was changed every 3 days. To increase the expression of MLC1 and GlialCAM detection at the plasma membrane (data not shown), we arrested astrocytic cultures in the cell cycle by addition of 2 μM cytosine β-D-arabinofuranoside (AraC, Sigma). Cultured astrocytes were identified by their positive GFAP staining (Dako).

Construction of adenovirus expressing wild-type HA-tagged human MLC1 has been described.[13] In a similar manner, we constructed and produced adenoviruses expressing three copies of the flag epitope fused to wild-type human GlialCAM or to human GlialCAM containing either the recessive mutations p.Arg92Gln, p.Arg98Cys, and p.Ser196Tyr or the dominant mutations p.Arg92Trp and p.Gly89Asp.

To infect astrocytes, we added adenoviruses at multiplicity of infection (MOI) 3 and kept them overnight at 37°C. Cells were washed, and then fresh medium was added. Astrocytes were incubated at 37°C until they were processed.

Results

MLC1-Interacting Proteins

We used a method of quantitative proteomic analysis of affinity-purified MLC1 to identify candidate genes for MLC. Independent affinity-purification experiments with MLC1 were performed with solubilized brain membranes and three different antibodies directed against peptides from the MLC1 N terminus (Figure 1A). Protein abundance determined by quantitative mass spectrometry identified HepaCAM, more correctly called GlialCAM,[18] as the protein with the second highest yield (after MLC1) in all purifications (Figure 1B and Figure S2A). Immunoblots with antibodies against GlialCAM (Figure S3) demonstrated that the protein was present in all purifications with all different MLC1 antibodies (Figure 1C). Not all GlialCAM coimmunoprecipitated with MLC1 (Figure 1C), possibly because not all GlialCAM is associated with MLC1 or because the coassembly dissolves during membrane protein solubilization. We confirmed the interaction between GlialCAM and MLC1 in reverse affinity purification experiments by using an antibody against GlialCAM that specifically coimmunoprecipitated GlialCAM and MLC1 from brain membranes. In the reverse purification, nearly all MLC1 was associated with GlialCAM (Figure 1D). Coimmunoprecipitation experiments with extracts from cells transfected with both genes also showed positive interaction (Figure S2B), indicating a direct interaction between the proteins. These findings made *HEPACAM* an excellent candidate gene for MLC patients without *MLC1* mutations.

HEPACAM Mutations in MLC Patients without *MLC1* Mutations

We analyzed the exons and surrounding intronic regions of *HEPACAM* in 40 patients from 34 families from around the world. In ten patients from eight families, we found two *HEPACAM* mutations (Table 1). Sequence analysis of *HEPACAM* in the parents showed autosomal-recessive inheritance of the two mutations in all cases except for one family with a de novo mutation. None of the patients had two mutations that abrogate expression of GlialCAM. In 18 patients from 16 families, we found one *HEPACAM* mutation, which was either inherited from a parent or arose de novo (Table 1). In 12 patients from ten families, we did not find *HEPACAM* mutations.

The observed nucleotide changes in *HEPACAM* are most likely pathogenic. They were not observed in 400 control chromosomes. All missense mutations affect amino acids that are conserved across a wide range of species (Figure 2B). Nine missense mutations affect amino acids in the predicted immunoglobulin domains in the extracellular part of GlialCAM (Figures 2A and 2C). p.Pro148Ser affects a residue between the two immunoglobulin domains. All these amino acid substitutions are predicted to affect protein function (SIFT). The substitution of residue Leu23 by His is predicted to affect the signal peptide, which spans the first 33 amino acids (SignalP 3.0 Server). Patient EL775 had two missense mutations, both inherited from the father. p.Asp128Asn is probably the pathogenic mutation because it is also observed in patients EL158 and EL708.

In 12 patients from ten families, neither *MLC1* nor *HEPACAM* mutations were found. In these families, we could not exclude linkage with both the *MLC1* and *HEPACAM* loci with certainty (data not shown). The possibility of hidden *MLC1* or *HEPACAM* mutations cannot, therefore, be excluded, and it is not certain that there must be a third gene mutated in MLC.

Table 1. *HEPACAM* Mutations

Patient	Exon	DNA	Protein	P/M/de novo[a]
Two Mutations				
EL84/85	3	c.587C>A	p.Ser196Tyr	P[b]
	4	c.789G>A	p.Trp263X	M
EL106	3	c.580 delC, 582C>T (hom)	p.Leu194PhefsX60	P + M
EL125	3	c.442C>T (hom)	p.Pro148Ser	***P*** + M
EL726	2	c.275G>A	p.Arg92Gln	P
	3	p.631G>A	p.Asp211Asn	M
EL774	2	c.292C>T (hom)	p.Arg98Cys	–[c]
EL785	1	c.68T>A	p.Leu23His	de novo
		c.461_462 del	p.Ser154TyrfsX16	***P***[d]
	4	c.742G>T	p.Gly248X	***P***[d]
EL816	3	c.442C>T (hom)	p.Pro148Ser	P+M
EL889/890	2	c.292C>T (hom)	p.Arg98Cys	P+M
One Mutation				
EL128	2	c.265G>A	p.Gly89Ser	de novo
EL158	2	c.382G>A	p.Asp128Asn	***P***[e]
EL604	2	c.265G>A	p.Gly89Ser	***P***
EL611	2	c.274C>T	p.Arg92Trp	***M***
EL624/625	2	c.274C>T	p.Arg92Trp	***M***
EL683/684	2	c.265G>A	p.Gly89Ser	***P***
EL686	2	c.266G>A	p.Gly89Asp	***P***
EL700	2	c.274C>T	p.Arg92Trp	–
EL708	2	c.382G>A	p.Asp128Asn	–
EL743	2	c.274C>T	p.Arg92Trp	M
EL775	2	c.382G>A	p.Asp128Asn	P[d]
	5	c.862C>T	p.Arg288Cys	P[d]
EL847	2	c.404_406 del	p.Lys135 del	***P***
EL862	2	c.265G>A	p.Gly89Ser	***M***
EL882	2	c.265G>A	p.Gly89Ser	de novo
EL903	2	c.265G>A	p.Gly89Ser	***M***[e]
EL944	2	c.274C>T	p.Arg92Trp	de novo

[a] P, paternal; M, maternal; bold and italic indicates macrocephaly.
[b] Probably from father but no DNA available.
[c] No DNA of the parents available.
[d] Both changes from same parental allele.
[e] Transient macrocephaly.

Inheritance, Phenotypes, and Mutations

All ten patients with two *HEPACAM* mutations inherited in an autosomal-recessive fashion had the classical phenotype (Table S2). They had infantile-onset macrocephaly and delayed-onset motor deterioration, epilepsy, and cognitive decline of variable severity. The MRI showed typical white matter abnormalities in all stages of the disease (Figure S1). The parents were normal, but two of the 16 had macrocephaly (Table 1).

All 18 patients with one *HEPACAM* mutation had the improving phenotype (Table S3). They developed macrocephaly within the first year. In two of the 18, the head circumference subsequently normalized. The motor capabilities became normal or almost normal. Some patients had normal intelligence, and others, with intelligence quoficients (IQs) between 50 and 75, had a stable mental retardation. Three of the mentally retarded patients also had autism or pervasive developmental disorder not otherwise specified according to DSM IV criteria. In summary, 11 of the 18 patients became clinically normal, apart from macrocephaly. MRI initially showed typical abnormalities but, on follow up, major improvement or normalization (Figure S1). For 13 patients from 11 families, eight of the 11 parents with the mutated allele had macrocephaly, one had transient macrocephaly as a child, and two never had macrocephaly as far as they could remember. Regarding the five remaining patients, the *HEPACAM* mutation arose de novo in three, and their parents had normal head circumference; DNA of the parents was not available in two. Only one of the parents without the mutated allele had macrocephaly. The family data suggest autosomal-dominant inheritance for the single *HEPACAM* mutations with variable penetrance. An analysis of microsatellite markers near *HEPACAM* in the families with the two most common dominant mutations (p.Gly89Ser and p.Arg92Trp) revealed no shared haplotype, excluding the possibility of founder effects for these two mutations (data not shown).

The *HEPACAM* mutations were either recessive or dominant. The recessive mutations were spread over the extracellular region of GlialCAM, whereas the dominant mutations were clustered in one of the predicted immunoglobulin-like domains (Figure 2C). Molecular modeling of the extracellular domain of GlialCAM showed that dominant mutations are located in a putative interface of the first immunoglobulin domain (Figure 2D).

GlialCAM-MLC1 Interaction

Immunohistochemistry of human brain tissue demonstrated GlialCAM expression mainly around blood vessels (Figure 3 and Figure S3). Double immunostaining with a monoclonal antibody against GlialCAM and a polyclonal antibody against human MLC1[13] showed that MLC1 and GlialCAM colocalize at astrocytic end-feet (Figure 3A). Immunogold EM confirmed this colocalization in astrocyte-astrocyte junctions (Figure 3B).

GlialCAM mRNA and protein have been detected in oligodendrocytes, astrocytes,[18] and neurons[19] (Figure S3), whereas MLC1 has not been detected in oligodendrocytes.[5–7,20] In MLC, vacuolation mainly affects the outer layers of myelin sheaths.[2] We investigated whether GlialCAM is localized in myelin. EM immunogold revealed

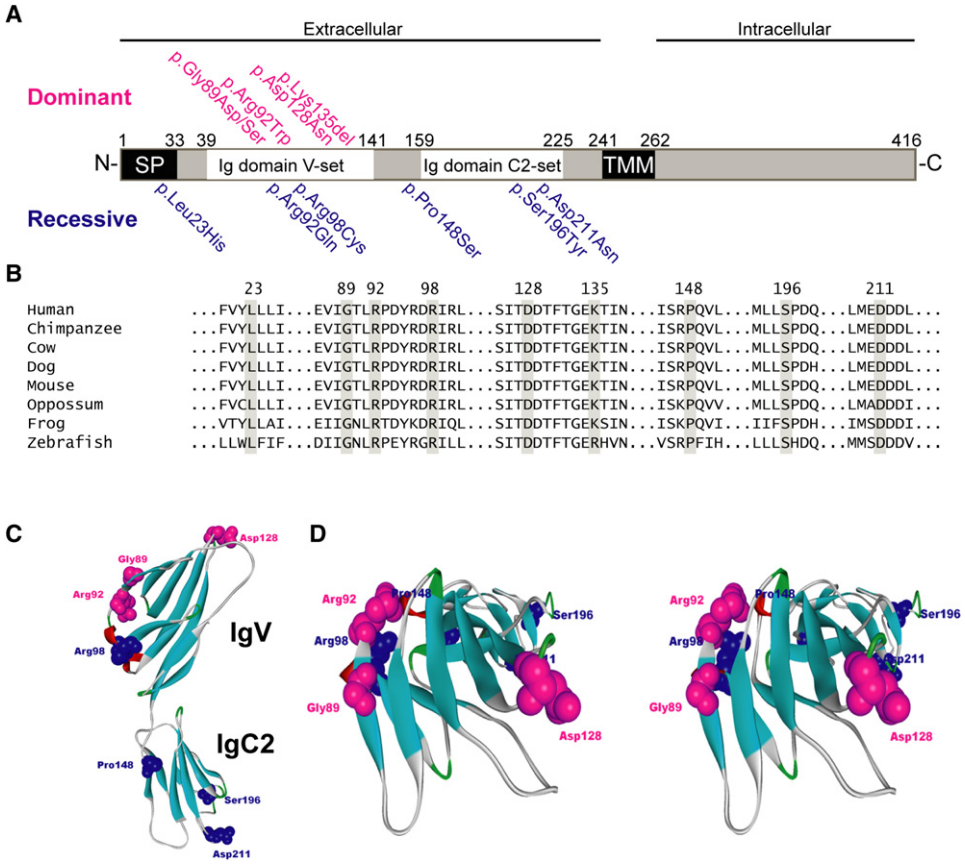

Figure 2. Genetic Studies in MLC Patients

(A) Schematic representation of domains in GlialCAM and position of missense mutations. The positions of several domains in human GlialCAM were predicted with PFAM, SOSUI, and SignalP 3.0. The following abbreviations are used: SP, signal peptide; TMM, transmembrane domain; Ig, Immunoglobulin. The missense mutations found in MLC patients are indicated above (dominant, in pink) and below (recessive, in blue) the figure.

(B) Conservation of affected amino acids. GlialCAM protein sequences were aligned with ClustalW software. The amino acids affected by missense mutations are indicated by a gray bar. The position of the affected residues in the human sequence is given above the sequences. NCBI accession numbers: *Homo sapiens*, NP_689935.2; Pan troglodytes, XP_522240.2; Bos taurus, NP_001026929.1; Canis familiaris, XP_852267.1; Mus musculus, NP_780398.2; Monodelphis domestica, XP_001371494.1; Danio rerio, NP_001018526.1. Ensembl protein ID: *Xenopus tropicalis*, ENSXETP00000008539.

(C) Schematic model of the protein GlialCAM. The structural model of the extracellular domain was accomplished with the automated homology-modeling server of the ExPASy server. Mutated residues are depicted with the same color-code as in (A).

(D) Stereo view of a ribbon representation viewed from the top of a structural model of the extracellular domain of GlialCAM. Pink highlights the residues mutated in dominant MLC, and blue highlights the residues in recessive MLC. Dominantly mutated residues are located in the putative extracellular-binding pocket, suggesting that it might mediate protein-ligand interactions.

particles inside axons, in contact regions between myelin and axons, and surrounding myelin (arrows in Figure 3C). In human medulla oblongata sections, where axons and myelin can be observed easily, immunostainings combining antibodies against GlialCAM with antibodies against neurofilament heavy chain (NF-H) or myelin basic protein (MBP) demonstrated that GlialCAM and NF-H staining coincide in axons (Figures 3D and 3E) and that not only is GlialCAM observed on the outside of myelin sheaths (inset in Figure 3E), but there is also a weak colocalization with MBP in myelin (Figure 3F). Classical biochemical fractionation protocols to purify myelin[14] and immunoblotting to detect specific proteins revealed GlialCAM but not MLC1 in the myelin fraction (Figure 3G).

The effect of mutations located in the extracellular domain of GlialCAM was studied in cultures of primary astrocytes, the cell type with the highest natural abundance of both MLC1 and GlialCAM. After adenoviral-mediated expression, lysates of astrocytes were analyzed by immunoblot and immunofluorescence. Expression levels of all types of mutant GlialCAM were not statistically different from wild-type GlialCAM (Figure S4). Immunofluorescence revealed that MLC1 and GlialCAM are located in cell-cell junctions between astrocytes (Figure 4A). Coexpression of wild-type MLC1 and GlialCAM containing the recessive mutations p.Arg92Gln or p.Arg98Cys resulted in diffuse intracellular MLC1 and GlialCAM localization with partial enrichment in cell membranes but not specifically in cell junctions (Figure 4B and Figure S5A). No defect

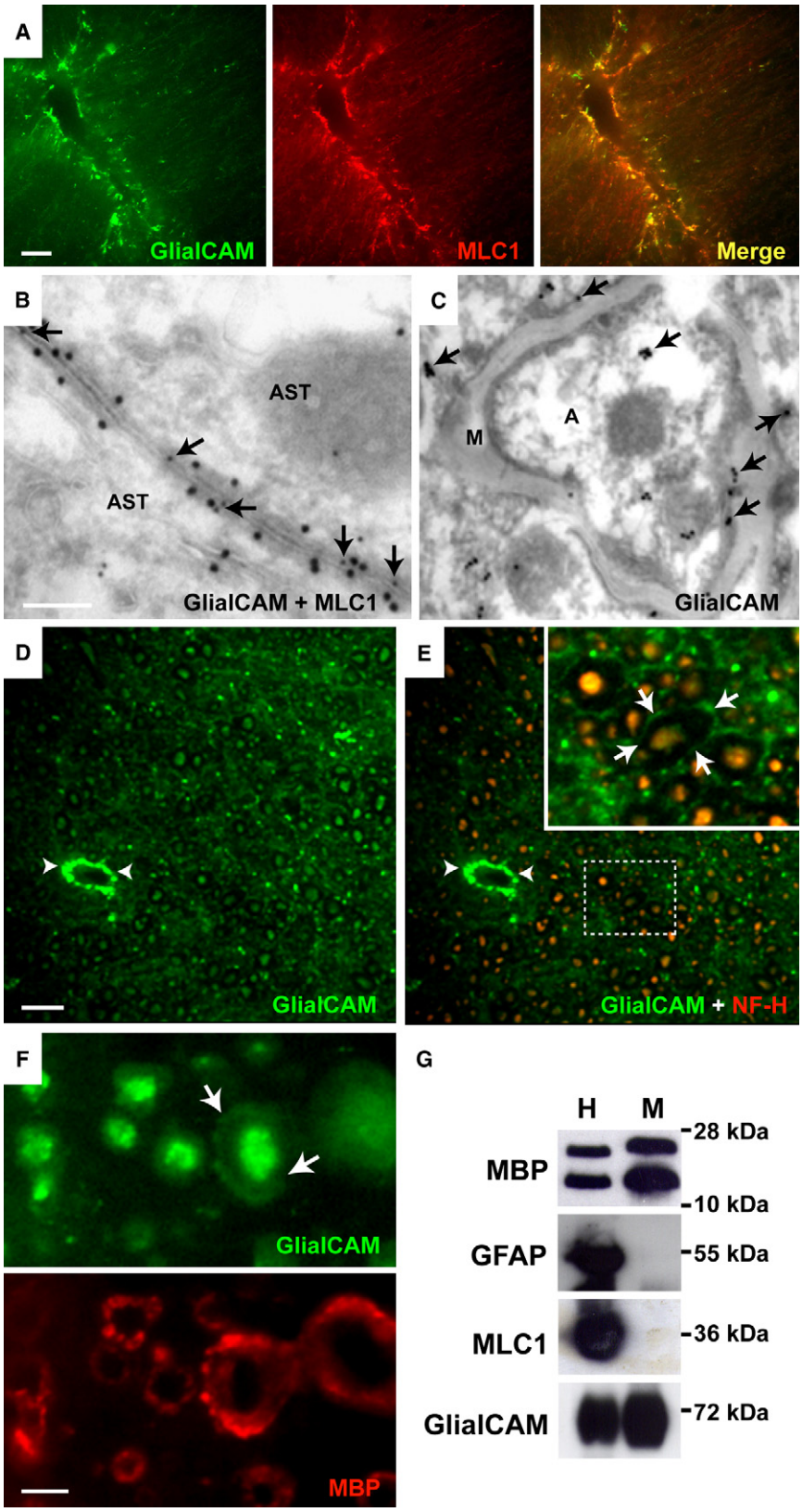

Figure 3. Colocalization of MLC1 and GlialCAM in Brain Tissue

(A) Double-immunolabeling experiments in human cerebellum, combining GlialCAM (in green) with MLC1 (in red), shows nearly complete colocalization (Merge, in yellow) in astrocytic processes surrounding a blood vessel.

(B) Double-immunolabeling EM shows colocalization of MLC1 (18 nm gold particles) and GlialCAM (with a commercially available monoclonal antibody; 12 nm gold particles, arrows) in astrocyte-astrocyte junctions in human tissue.

(C) Postembedding staining of GlialCAM in human cerebellum also shows immunoreactivity (arrows) inside axons, in contact regions between myelin and axons, and in cells that surround myelin.

(D–F) Localization of GlialCAM in human medulla oblongata. Using the polyclonal rabbit antibody, we detected GlialCAM in astrocytes surrounding blood vessels (arrowheads in D and E), in axons, and in myelin (arrows in inset in E and in F). Double immunolabeling of GlialCAM and NF-H, which stains axons, confirmed colocalization of GlialCAM and NF-H (yellow staining in E). The dashed line in E indicates the area amplified in the inset. Double immunolabeling of GlialCAM and MBP, which stains myelin, demonstrated a weak labeling of GlialCAM in myelin.

(G) Myelin was purified from brains of 6- to 8-month-old mice as described in the Material and Methods. Twenty microgram of the initial homogenate (H) and of myelin (M) were analyzed by SDS-PAGE and immunoblotting. Blots were probed with antibodies against MBP, GFAP, MLC1, and GlialCAM. The amount of GFAP detected in the myelin fraction was low as compared to the homogenate, indicating that the contamination of the myelin fraction with nonmyelin proteins was low. The following abbreviations are used: AST, astrocyte; MBP, myelin basic protein; GFAP, glial fibrillary acid protein; NF-H, neurofilament heavy chain; M, myelin; A, axon.

The scale bars indicate 50 μm (A and D), 500 nm (B and C), and 10 μm (F).

was found for the mutation p.Ser196Tyr (Figure S5C). Similar mislocalization of MLC1 and GlialCAM was observed after coexpression of wild-type MLC1 and GlialCAM containing the dominant mutations p.Arg92Trp and p.Gly89Asp (Figures 4D and Figure S5D).

To address the mode of inheritance of the mutations biochemically, we performed experiments with equal levels of wild-type GlialCAM and GlialCAM containing a dominant or recessive mutation together with MLC1. The localization of MLC1 and GlialCAM was analyzed by immunofluorescence. Coexpression of wild-type GlialCAM rescued the MLC1-trafficking defect caused

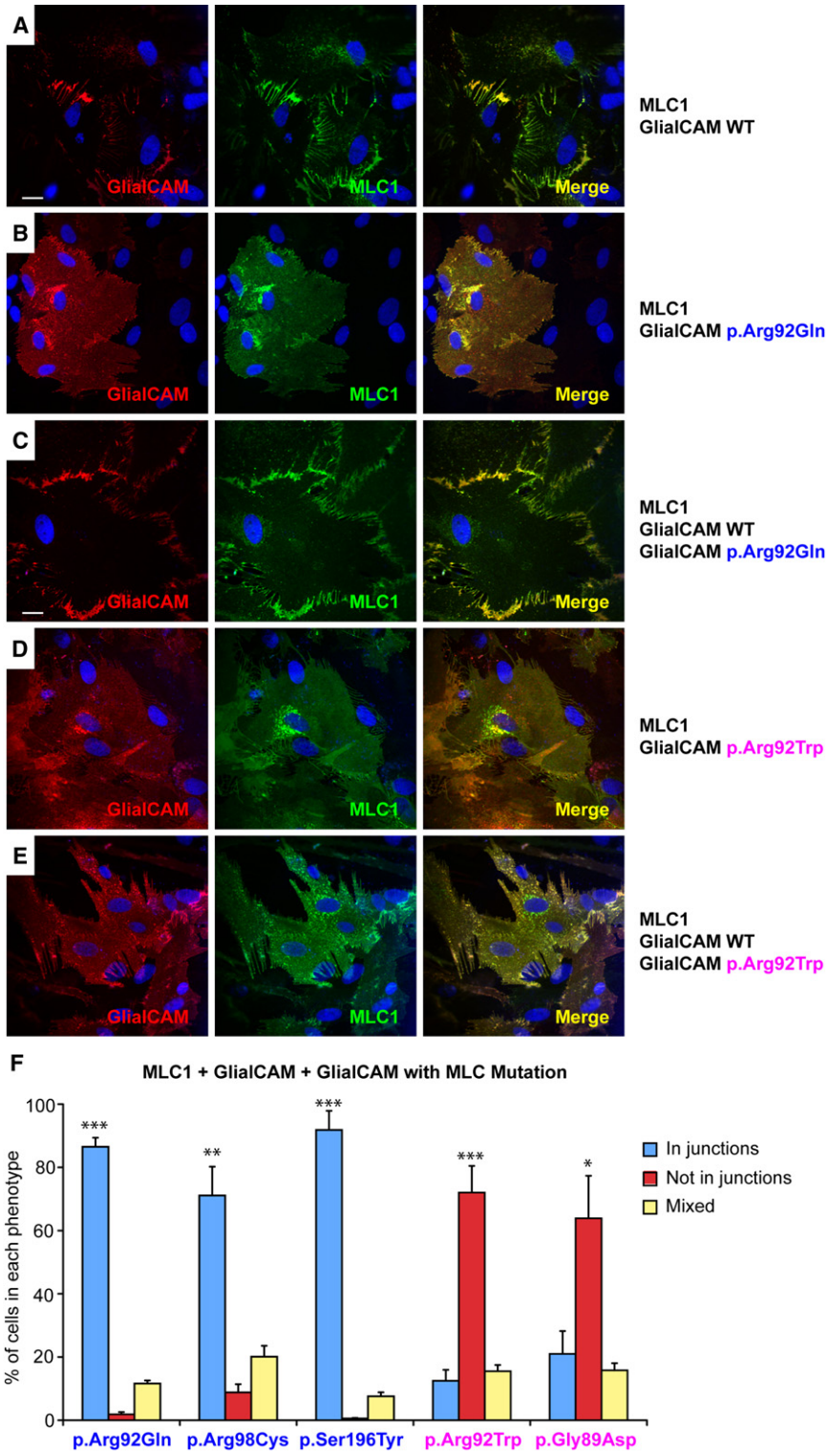

Figure 4. MLC1 and GlialCAM Subcellular Localization Changes Caused by Recessive and Dominant GlialCAM Mutations in Primary Cultures of Astrocytes

(A–F) Astrocytes were coinfected with adenoviruses expressing MLC1 and wild-type GlialCAM (A) or GlialCAM containing a recessive (B, p.Arg92Gln) or a dominant (D, p.Arg92Trp) MLC-related mutation at MOI 3. In (C) and (E), cells were coinfected with MLC1, wild-type GlialCAM, and GlialCAM containing the indicated mutation at a MOI ratio of 3:2:2. Cells were fixed, and permeabilized and then immunofluorescence was performed with a rabbit polyclonal antibody against human MLC1 (green) and a monoclonal antibody detecting GlialCAM protein (red). Nuclei were stained with DAPI (blue). Colocalization between the green and the red channel is shown in yellow. Images correspond to representative cells from four independent experiments. The scale bars represent 20 μm. (F) Random pictures from different experiments were taken. Quantification of the percentage of cells located in junctions (blue), not in junctions (red), or with a mixed phenotype (yellow, located partially in junctions and not in junctions) was performed manually. Data are mean ± standard error of the mean of four independent experiments. Bonferroni's multiple comparison test versus in junctions and not in junctions was used. *$p < 0,05$; **$p < 0,01$; ***$p < 0,001$. Representative images for the other mutations shown in the quantification are depicted in Figure S5.

by GlialCAM with recessive mutations (Figures 4C and 4F and Figure S5B) but did not rescue the trafficking defect caused by GlialCAM with dominant mutations (Figures 4E and 4F and Figure S5E). No difference in protein levels was observed between the mutants and the wild-type (Figure S4), making it unlikely that the trafficking defect is due to gene-dosage effects.

Discussion

The leukodystrophy MLC is characterized by infantile-onset macrocephaly and delayed neurological deterioration. The diagnosis is based on MRI criteria.[1] In 2001, causative mutations of MLC were identified in *MLC1*, accounting for approximately 75% of the patients. The fact that genetic-linkage studies failed to identify a second gene was ascribed to further genetic heterogeneity.[9,10] We recently identified two presumably autosomal recessive, phenotypes among MLC patients without *MLC1* mutations,[11] corroborating the notion of genetic heterogeneity. We now show that the genetic heterogeneity does not involve the gene but the mode of inheritance. We circumvented the problem of genetic heterogeneity by using a proteomic approach. This method is validated by the discovery of *HEPACAM* (hepatic and glial cell adhesion molecule, MIM 611642) as a gene disrupted in MLC and

can be considered in the future to identify disease genes for other rare or genetically heterogeneous disorders.

We prefer the name GlialCAM above HepaCAM for the related protein. Although the protein was first isolated from liver and called HepaCAM,[21] it was subsequently found to be predominantly expressed in the central nervous system and was renamed GlialCAM.[18] In the present paper, we show that mutations in *HEPACAM* lead to a neurological phenotype without any sign of liver involvement.

That mutations in one gene cause both autosomal-recessive and -dominant disease is rare but not unique. It has been described for a few other genes, including *LMNA* (MIM 150330), *SOX18* (MIM 601618), *ANK1* (MIM 612641), *COL6A1* (MIM 120220), *PMP22* (MIM 601097), and *MPZ* (MIM 159440).[22–27] However, patients with the dominant mutations in these genes do not display an improving phenotype, as seen in our MLC patients with dominant *HEPACAM* mutations. In MLC, the macrocephaly and cerebral white-matter disease on MRI arise in the first year of life, the period of most rapid myelin deposition in the brain. Apparently, MLC1 and GlialCAM exert their most important function during this process. The functions of both MLC1 and GlialCAM are unknown. We, therefore, do not understand the mechanism of the improving phenotype for the dominant *HEPACAM* mutations. A hypothetical gene-dose effect is not supported by the finding that normal GlialCAM does not partially rescue the localization of the GlialCAM-MLC1 complex in astrocytes expressing a dominant *HEPACAM* mutation. The dominant mutations are located in a putative pocket of the immunoglobulin domain and might disrupt interactions with GlialCAM itself and other unknown molecules.

GlialCAM acts as a MLC1 beta subunit needed for its correct trafficking to cell-cell junctions. Probably, *cis*- or *trans*-interactions mediated by GlialCAM are necessary for its correct localization. The function of GlialCAM as an adhesion molecule suggests that both GlialCAM and MLC1 have a role in the maintenance of correctly sealed cell-cell contacts. Interestingly, GlialCAM and not MLC1 is detected in myelin, the place where most vacuoles are found in MLC.[2] GlialCAM is not obligatorily associated with MLC1, indicating that it might have other functions by itself or in association with other molecules. Recently, it has been suggested that MLC1 interacts with the β1 subunit of the Na,K-ATPase pump.[28] We did not detect this protein in our affinity purifications. Further studies on MLC1-interacting proteins might provide better insights into the pathophysiology of MLC.

GlialCAM is an interesting protein. In 60% of the families with dominant *HEPACAM* mutations, the affected persons in fact display benign familial macrocephaly (MIM 153470). They have macrocephaly, but they are otherwise normal. MRI shows large but normal brains. The parents did not undergo MRI as children, and a transient leukoencephalopathy was not documented in any of them. Benign familial macrocephaly is most likely genetically heterogeneous, and *HEPACAM* is likely to be one of the related genes. Another interesting finding is that in 40% of the patients with a dominant *HEPACAM* mutation, macrocephaly, and mental retardation with or without autism, which are known to be associated features, persist.[29] This clinical syndrome is probably genetically heterogeneous, and specific *HEPACAM* mutations could cause it. The fact that single *HEPACAM* mutations might be associated with different phenotypes requires the geneticist to be cautious when counseling an affected family. From the age of approximately 2–3 years, the combination of clinical picture and MRI findings allows an accurate prediction of the phenotype.

In conclusion, we have found that *HEPACAM* is mutated in MLC. Recessive mutations cause a progressive leukodystrophy that is indistinguishable clinically and by MRI from the disease caused by recessive *MLC1* mutations. Dominant mutations can cause transient clinical and MRI features of MLC, benign familial macrocephaly, and the clinical syndrome of macrocephaly and mental retardation with or without autism.

Supplemental Data

Supplemental Data include five figures and three tables and can be found with this article online at http://www.cell.com/AJHG/.

Acknowledgments

Research in our laboratories was supported by Ministerio de Ciencia y Tecnología (SAF) 2009-07014 (R.E.), Fundación Ramon Areces project (R.E.), European Leukodystrophy Association Foundation 2007-017C4 project (R.E. and M.S.v.d.K.), PS09/02672-ERARE (R.E.), ERARE grant 11-330-1024 (G.C.S. and M.S.v.d.K.), 2009 Grups de Recerca de Catalunya 719 (R.E.), SAF 2009-12606-C02-02 (V.N.), CIBERER INTRA08/750 (R.E. and V.N.), and 2009 SGR01490 (V.N.). M.S.v.d.K., G.C.S., and M.C.R. are supported by the Dutch Organization for Scientific Research ZonMw (TOP Grant 9120.6002), the Hersenstichting (Grants 13F05.04, 15F07.30 and 2009[2]-14), and the Optimix Foundation for Scientific Research. R.E. is a recipient of an ICREA Academia prize. We thank all colleagues who contributed MRI, clinical information, and blood samples. We thank Alejandro Barrallo, Michael Pusch, and Jim M. Powers for critical review of the manuscript.

Received: December 7, 2010
Revised: January 12, 2011
Accepted: February 21, 2011
Published online: March 17, 2011

Web Resources

The URLs for data presented herein are as follows:

ExonPrimer, http://ihg.gsf.de/ihg/ExonPrimer.html
Online Mendelian Inheritance in Man, http://www.ncbi.nlm.nih.gov/Omim/
SIFT, http://sift.jcvi.org/

Signal P, http://www.cbs.dtu.dk/services/SignalP/
Swissmodel, http://swissmodel.expasy.org/

References

1. van der Knaap, M.S., Barth, P.G., Stroink, H., van Nieuwenhuizen, O., Arts, W.F., Hoogenraad, F., and Valk, J. (1995). Leukoencephalopathy with swelling and a discrepantly mild clinical course in eight children. Ann. Neurol. *37*, 324–334.
2. van der Knaap, M.S., Barth, P.G., Vrensen, G.F., and Valk, J. (1996). Histopathology of an infantile-onset spongiform leukoencephalopathy with a discrepantly mild clinical course. Acta Neuropathol. *92*, 206–212.
3. Leegwater, P.A., Yuan, B.Q., van der Steen, J., Mulders, J., Könst, A.A., Boor, P.K., Mejaski-Bosnjak, V., van der Maarel, S.M., Frants, R.R., Oudejans, C.B., et al. (2001). Mutations of MLC1 (KIAA0027), encoding a putative membrane protein, cause megalencephalic leukoencephalopathy with subcortical cysts. Am. J. Hum. Genet. *68*, 831–838.
4. Ilja Boor, P.K., de Groot, K., Mejaski-Bosnjak, V., Brenner, C., van der Knaap, M.S., Scheper, G.C., and Pronk, J.C. (2006). Megalencephalic leukoencephalopathy with subcortical cysts: An update and extended mutation analysis of MLC1. Hum. Mutat. *27*, 505–512.
5. Teijido, O., Martínez, A., Pusch, M., Zorzano, A., Soriano, E., Del Río, J.A., Palacín, M., and Estévez, R. (2004). Localization and functional analyses of the MLC1 protein involved in megalencephalic leukoencephalopathy with subcortical cysts. Hum. Mol. Genet. *13*, 2581–2594.
6. Boor, P.K.I., de Groot, K., Waisfisz, Q., Kamphorst, W., Oudejans, C.B., Powers, J.M., Pronk, J.C., Scheper, G.C., and van der Knaap, M.S. (2005). MLC1: A novel protein in distal astroglial processes. J. Neuropathol. Exp. Neurol. *64*, 412–419.
7. Teijido, O., Casaroli-Marano, R., Kharkovets, T., Aguado, F., Zorzano, A., Palacín, M., Soriano, E., Martínez, A., and Estévez, R. (2007). Expression patterns of MLC1 protein in the central and peripheral nervous systems. Neurobiol. Dis. *26*, 532–545.
8. Kaganovich, M., Peretz, A., Ritsner, M., Bening Abu-Shach, U., Attali, B., and Navon, R. (2004). Is the WKL1 gene associated with schizophrenia? Am. J. Med. Genet. B. Neuropsychiatr. Genet. *125B*, 31–37.
9. Blattner, R., Von Moers, A., Leegwater, P.A., Hanefeld, F.A., Van Der Knaap, M.S., and Köhler, W. (2003). Clinical and genetic heterogeneity in megalencephalic leukoencephalopathy with subcortical cysts (MLC). Neuropediatrics *34*, 215–218.
10. Patrono, C., Di Giacinto, G., Eymard-Pierre, E., Santorelli, F.M., Rodriguez, D., De Stefano, N., Federico, A., Gatti, R., Benigno, V., Megarbané, A., et al. (2003). Genetic heterogeneity of megalencephalic leukoencephalopathy and subcortical cysts. Neurology *61*, 534–537.
11. van der Knaap, M.S., Lai, V., Köhler, W., Salih, M.A., Fonseca, M.J., Benke, T.A., Wilson, C., Jayakar, P., Aine, M.R., Dom, L., et al. (2010). Megalencephalic leukoencephalopathy with cysts without MLC1 defect. Ann. Neurol. *67*, 834–837.
12. Zolles, G., Wenzel, D., Bildl, W., Schulte, U., Hofmann, A., Müller, C.S., Thumfart, J.O., Vlachos, A., Deller, T., Pfeifer, A., et al. (2009). Association with the auxiliary subunit PEX5R/Trip8b controls responsiveness of HCN channels to cAMP and adrenergic stimulation. Neuron *62*, 814–825.
13. Duarri, A., Teijido, O., López-Hernández, T., Scheper, G.C., Barriere, H., Boor, I., Aguado, F., Zorzano, A., Palacín, M., Martínez, A., et al. (2008). Molecular pathogenesis of megalencephalic leukoencephalopathy with subcortical cysts: Mutations in MLC1 cause folding defects. Hum. Mol. Genet. *17*, 3728–3739.
14. Norton, W.T., and Poduslo, S.E. (1973). Myelination in rat brain: Method of myelin isolation. J. Neurochem. *21*, 749–757.
15. Pandey, A., Andersen, J.S., and Mann, M. (2000). Use of mass spectrometry to study signaling pathways. Sci. STKE *2000*, pl1.
16. Schwenk, J., Metz, M., Zolles, G., Turecek, R., Fritzius, T., Bildl, W., Tarusawa, E., Kulik, A., Unger, A., Ivankova, K., et al. (2010). Native GABA(B) receptors are heteromultimers with a family of auxiliary subunits. Nature *465*, 231–235.
17. McCarthy, K.D., and de Vellis, J. (1980). Preparation of separate astroglial and oligodendroglial cell cultures from rat cerebral tissue. J. Cell Biol. *85*, 890–902.
18. Favre-Kontula, L., Rolland, A., Bernasconi, L., Karmirantzou, M., Power, C., Antonsson, B., and Boschert, U. (2008). GlialCAM, an immunoglobulin-like cell adhesion molecule is expressed in glial cells of the central nervous system. Glia *56*, 633–645.
19. Spiegel, I., Adamsky, K., Eisenbach, M., Eshed, Y., Spiegel, A., Mirsky, R., Scherer, S.S., and Peles, E. (2006). Identification of novel cell-adhesion molecules in peripheral nerves using a signal-sequence trap. Neuron Glia Biol. *2*, 27–38.
20. Schmitt, A., Gofferje, V., Weber, M., Meyer, J., Mössner, R., and Lesch, K.P. (2003). The brain-specific protein MLC1 implicated in megalencephalic leukoencephalopathy with subcortical cysts is expressed in glial cells in the murine brain. Glia *44*, 283–295.
21. Chung Moh, M., Hoon Lee, L., and Shen, S. (2005). Cloning and characterization of hepaCAM, a novel Ig-like cell adhesion molecule suppressed in human hepatocellular carcinoma. J. Hepatol. *42*, 833–841.
22. Raffaele Di Barletta, M., Ricci, E., Galluzzi, G., Tonali, P., Mora, M., Morandi, L., Romorini, A., Voit, T., Orstavik, K.H., Merlini, L., et al. (2000). Different mutations in the LMNA gene cause autosomal dominant and autosomal recessive Emery-Dreifuss muscular dystrophy. Am. J. Hum. Genet. *66*, 1407–1412.
23. Irrthum, A., Devriendt, K., Chitayat, D., Matthijs, G., Glade, C., Steijlen, P.M., Fryns, J.P., Van Steensel, M.A., and Vikkula, M. (2003). Mutations in the transcription factor gene SOX18 underlie recessive and dominant forms of hypotrichosis-lymphedema-telangiectasia. Am. J. Hum. Genet. *72*, 1470–1478.
24. Eber, S.W., Gonzalez, J.M., Lux, M.L., Scarpa, A.L., Tse, W.T., Dornwell, M., Herbers, J., Kugler, W., Ozcan, R., Pekrun, A., et al. (1996). Ankyrin-1 mutations are a major cause of dominant and recessive hereditary spherocytosis. Nat. Genet. *13*, 214–218.
25. Lampe, A.K., and Bushby, K.M. (2005). Collagen VI related muscle disorders. J. Med. Genet. *42*, 673–685.
26. Roa, B.B., Garcia, C.A., Pentao, L., Killian, J.M., Trask, B.J., Suter, U., Snipes, G.J., Ortiz-Lopez, R., Shooter, E.M., Patel, P.I., and Lupski, J.R. (1993). Evidence for a recessive PMP22 point mutation in Charcot-Marie-Tooth disease type 1A. Nat. Genet. *5*, 189–194.
27. Nicolaou, P., Zamba-Papanicolaou, E., Koutsou, P., Kleopa, K.A., Georghiou, A., Hadjigeorgiou, G., Papadimitriou, A.,

Kyriakides, T., and Christodoulou, K. (2010). Charcot-Marie-Tooth disease in Cyprus: Epidemiological, clinical and genetic characteristics. Neuroepidemiology *35*, 171–177.

28. Brignone, M.S., Lanciotti, A., Macioce, P., Macchia, G., Gaetani, M., Aloisi, F., Petrucci, T.C., and Ambrosini, E. (2011). The beta1 subunit of the Na,K-ATPase pump interacts with megalencephalic leucoencephalopathy with subcortical cysts protein 1 (MLC1) in brain astrocytes: New insights into MLC pathogenesis. Hum. Mol. Genet. *20*, 90–103.
29. White, S., O'Reilly, H., and Frith, U. (2009). Big heads, small details and autism. Neuropsychologia *47*, 1274–1281.